

A PERTURBED TRI-POLYTROPIC MODEL OF THE SUN

Pinzón G.¹ Calvo-Mozo B.²

*Observatorio Astronómico Nacional, Universidad Nacional de Colombia
A.A. 2584, Bogotá 1, Colombia*

ABSTRACT

Based on the Solar Standard Model SSM of Bahcall and Pinsonneault (SSM-BP2000) we developed a solar model in hydrostatic equilibrium using three polytropes, each one associated to the *nuclear*, the *radiative* and the *convective* regions of the solar interior. Then, we apply small periodic and adiabatic perturbations on this tri-polytropic model in order to obtain proper frequencies and proper functions which are in the **p-modes** range of low order $0 < l < 5$; for $l = 2, 3$ and 4 these values agrees with **GOLF** observational data within a few percent.

Subject headings: Solar Standard Model (SSM), Lane-Emden, Non Radial Oscillations (NRO), p-modes

1. Introduction

Polytropic models have largely been used in the study of NRO of a gaseous sphere [Cowling,1941; Kopal,1949; Scuflaire,1974; Tassoul,1980].

We have computed the first modes of a tri-polytropic model (**TPM**) whose indices $n_1 = 1.50$, $n_2 = 3.78$ and $n_3 = 20$ describes the *convective*, *radiative* and *nuclear* zones respectively of the solar interior. We used Cowling's approximation [Cowling,1941] which reduces the order of the system of differential equations to 2 (instead of 4). The radial part of the perturbation obeys equations (1) and (2) [Ledoux-Walraven,1958]:

$$\frac{dv}{dr} = \left[\frac{L_l^2}{\sigma^2} - 1 \right] \frac{P^{\frac{2}{\Gamma_1}}}{\rho} w \quad (1)$$

$$\frac{dw}{dr} = \frac{1}{r^2} [\sigma^2 - N^2] \frac{\rho}{P^{\frac{2}{\Gamma_1}}} v \quad (2)$$

where

$$v = r^2 \delta r P^{\frac{1}{\Gamma_1}} \quad (3)$$

$$w = \frac{P'}{P^{\frac{1}{\Gamma_1}}} \quad (4)$$

are proper functions, l is the degree of the spherical harmonic, Γ_1 is the adiabatic exponent equal

to $\frac{5}{3}$, σ is the angular frequency, N is the *Brunt-Väisälä* frequency and L_l is the *Lamb* frequency.

The equations (1) and (2) and the boundary conditions lead to a eigenvalue problem with eigenvalue σ^2 , which is the problem to be solved.

2. Polytropes

Our unperturbed model consist of a gas of particles with spherical symmetry, selfgravitating, in hydrostatic equilibrium and with its state equation given by:

$$P = K \rho^\gamma = K \rho^{1+\frac{1}{n}} \quad (5)$$

K and γ are parameters that depend only on the polytropic index n , and the mass and radius of the configuration. The polytrope theory developed by the ends of the XIX century, can be used to know the dynamical structure of a star, within which local quasistatic thermodynamic changes follows a *polytropic process*, i.e. one in which the specific heat remains constant. This approach can be used in some regions of Sun's interior. We have used the pressure and the density data from the sophisticated SSM of Bahcall and Pinsonneault to plot $\gamma = \frac{d \ln P}{d \ln \rho}$ vs x with $x = r/R_\odot$. Various regions clearly emerge. Of these regions, the outermost one ($\gamma_1 = 1.677$, i.e. $n_1 = 1.50$) represents the *convective* zone where heat transport is achieved by adiabatic convection. It's SSM output in *Fig.1* is approximated rather well by a constant

¹e-mail gpinzon@ciencias.unal.edu.co

²e-mail bcalvo@ciencias.unal.edu.co

straight line indicating a polytropic behavior. The second intermediate zone labeled *radiative zone* in *Fig.1* can be approach by a polytrope $\gamma_2 = 1.264$, i.e. $n_2 = 3.788$. Finally, we have taken an average of γ for the innermost regions labeled *nuclear zone*, so we represent this zone by a polytrope with $\gamma_3 = 1.050$, i.e $n_3 = 20.0$. This three polytropes have been use by Hendry (1993).

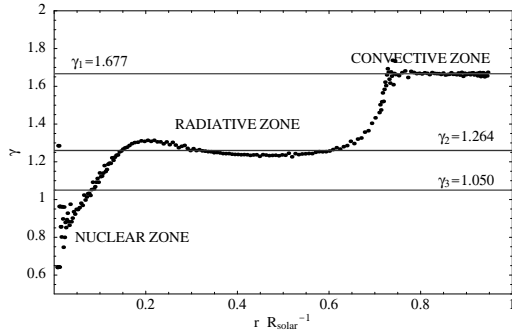


Fig. 1.— γ at the solar interior due to SSM [Bahcall and Pinsonneault,2000]. Regions with γ constant are described by polytropic process. The tri-polytropic model is obtained if one assume three values for γ ; $\frac{5}{3}$ in the *convective zone*, 1.264 in the *radiative zone* and 1.050 in the *nuclear zone*.

2.1. Three polytropes within the Sun

Following Hendry [Hendry, 1993] we use ξ , θ as the variables in the **Lane-Emden** equation for the *convective zone* with index n_1 ; η , ϕ as the variables for the *radiative zone* with index n_2 and ζ , ψ as the variables for the *nuclear zone* with index n_3 . Hence the parametric polytropes are:

$$P = K_1 \rho^{\frac{5}{3}}, \text{ with } \rho = \lambda_1 \theta(\xi)^{1.5} \quad (6)$$

$$P = K_2 \rho^{1.26}, \text{ with } \rho = \lambda_2 \phi(\eta)^{3.85} \quad (7)$$

$$P = K_3 \rho^{1.05}, \text{ with } \rho = \lambda_3 \psi(\zeta)^{20} \quad (8)$$

The main challenge is to learn how to fit these three polytropes together. Since the physical quantities P , ρ and M are continuous across the interfaces (not for example θ or ϕ), the variables U and V given by

$$U = \frac{\xi \theta^n}{-\theta'} \quad (9)$$

$$V = \frac{(n+1)\xi(-\theta')}{\theta} \quad (10)$$

are be very useful [Chandrasekhar,1939].

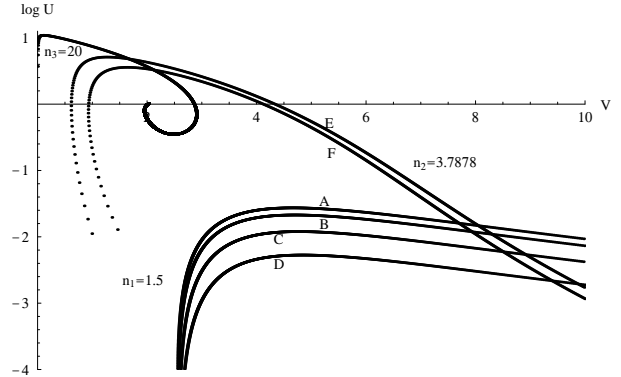


Fig. 2.— Solutions of the **Lane-Emden** equation. The center of the Sun as at $V = 0$, $U = 3$ and its surface at $U = 0$, $V = \infty$. We choose $\theta'_{\xi_1} = -0.00325$ (curve C) as a **M-Solution** for the *convective zone* and $\phi'_{\eta_1} = -0.0117$ (curve E) as a **M-Solution** for the *radiative zone*.

Let us start by considering the *convective zone*. We take $n_1 = 1.5$ thus $\xi_1 = 3.6538$ and $\theta'_{\xi_1} = -0.2033$. Though, this polytrope is not being used in the vicinity of $\xi = 0$, it is possible to consider all of the solutions of the **Lane-Emden** equation for $n_1 = 1.50$. These may be generated beginning at ξ_1 with an arbitrary starting slope and integrating inwards. Solutions with starting slopes less negative than θ'_{ξ_1} are of particular interest (in the literature, they are referred to as **M-solutions**) since these are the ones which intersect the polytrope that represents the *radiative zone* $n_2 = 3.788$. Four such solutions, translated into the U , V variables, are shown in *Fig.2*, as the curves A, B, C and D there. Solutions with starting slopes more negative than θ'_{ξ_1} (**F-solutions**) do not intersect the *radiative* polytrope and so do not need to be considered here. In the same way we have worked the intersection between the *nuclear* and *radiative* zones; we have fixed the *nuclear* polytrope with the θ_{20} **E-solution** which intersects the **M-solutions** (*Fig.2*, as curves E and F) that represents the *radiative zone* $n_2 = 3.788$, this occur at the neighbors to $0.25R_{\odot}$.

Knowing $\theta(\xi)$, $\phi(\eta)$ and $\psi(\zeta)$ we can deduce the density and pressure curves $\rho(r)$ and $P(r)$. The above model yields a central density³ of $\rho_c = 1.483 \times 10^5 \text{ Kg m}^{-3}$ in comparison with $\rho_c = 1.299 \times 10^5 \text{ Kg m}^{-3}$ obtained for the bi-polytropic

³SSM value: $1.524 \times 10^5 \text{ Kg m}^{-3}$ [Bahcall and Pinsonneault,2000]

model **BPM** [Pinzón-Calvo-Mozo,2001].

A comparison of our **BPM** and **TPM** models with the **SSM-BP2000** are shown in *Fig.3*, showing a better fit of the **TPM** with respect to the **SSM-BP2000** in the most central part.

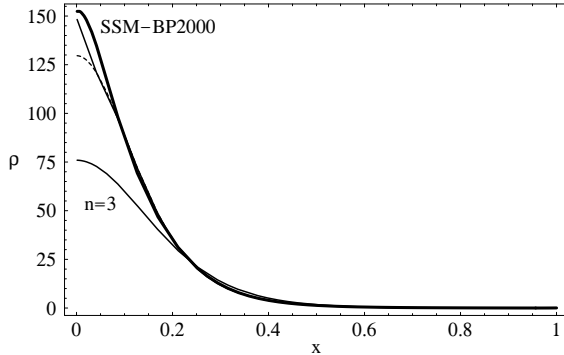


Fig. 3.— Density (in $g \times cm^{-3}$) at the solar interior for **TPM** (thin line), for the **BPM** (dashed line), for the **SSM-BP2000** (thick line) and for the $n = 3$ one polytrope model.

2.2. Characteristic Frequencies

The characteristic N and L frequencies so called *Brunt-Väisälä* and *Lamb* frequencies associated with restoring forces of pressure and gravity in a polytrope of order n can be calculated as functions of radius in terms of the Lane-Emden function θ . Thus, if we define:

$$\omega_g = \frac{GM_\odot}{R_\odot^3} \quad (11)$$

where R_\odot and M_\odot are the sun mass and the sun radius, and G is the gravitational constant, we can write a normalized *Brunt-Väisälä* frequency as:

$$N_n^2 \equiv \frac{N^2}{\omega_g} = \frac{(n - n_0)}{(n_0 + 1)} \times CC \times \frac{3}{\theta} \left(\frac{d\theta}{d\xi} \right)^2 \quad (12)$$

where CC is the central condensation of the polytrope, defined as the ratio of central density to mean density. The parameter n_0 is the effective polytropic index associated to the pulsations [Mullan-Ulrich,1988], which in turns related to the adiabatic exponent⁴ Γ by:

⁴We supposed $\Gamma = \frac{5}{3}$.

$$\Gamma = 1 + \frac{1}{n_0} \quad (13)$$

Similarly, the value of the *Lamb* frequency associated to the mode l is given by:

$$L_{ln} \equiv \frac{L_l^2}{\omega_g} = 3 \times CC \times l(l+1) \times \frac{\theta}{\xi^2} \times \frac{n_0 + 1}{n_0(n+1)} \quad (14)$$

where ξ is the Lane-Emden coordinate.

3. NRO in a Tri-polytropic Model (TPM)

Space oscillation properties of the solutions of equations (1) and (2) are related to the signs of the coefficients given by the second members of these equations. Space oscillations are allowed only in the regions where these coefficients have opposite signs. The limits of these regions are defined by

$$\sigma^2 = \frac{l(l+1)\Gamma_1 P}{\rho r^2} = L_l^2 \quad (15)$$

$$\sigma^2 = N^2 \quad (16)$$

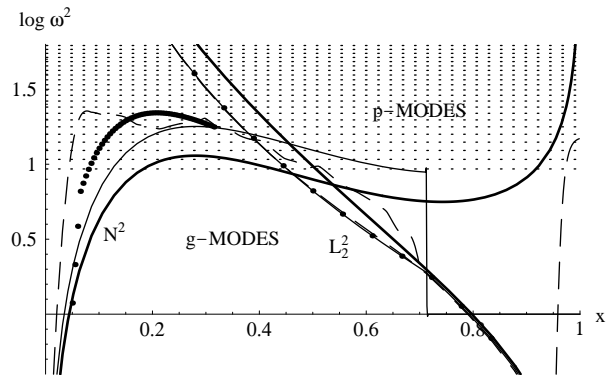


Fig. 4.— **Propagation Diagram** ($l = 2$) for the **BPM** (thin lines), for the polytropic index 3 model (thick lines) and for the **SSM-BP2000** (dashed lines). The **TPM** agree exactly to the **BPM** except near the center; in this region some points for the **TPM** are shown.

In the (x, ω^2) plane, these equations define two curves. In *Fig.4* we have plotted (15) and (16) as thin black curves for the **BPM**. We can see that the *Lamb* frequency diverges near to the center; conversely, the *Brunt-Väisälä* runs from zero at

the origin and diverges near the surface. This feature is common in all models. The **TPM** propagation diagram is very similar to **BPM** except at the nuclear region, where there is a prominent change. We have been denoted *p-modes* and *g-modes* the regions of (x, ω^2) plane corresponding to the conditions of position and frequency in the star, allowing spatial oscillations. These regions are characterized by the possibility of existence of progressive acoustic waves and progressive gravity waves respectively [Scuflaire,1974]. Thus we shall refer to these regions as the acoustic and the gravity regions. We have also plotted in the same figure the frequencies (horizontal dot lines) for the first *p-modes* from *p12 - mode* for the **TPM**. In addition in the same figure, we can see the propagation diagram for the **SSM** [Bahcall and Pinsonneault,2000].

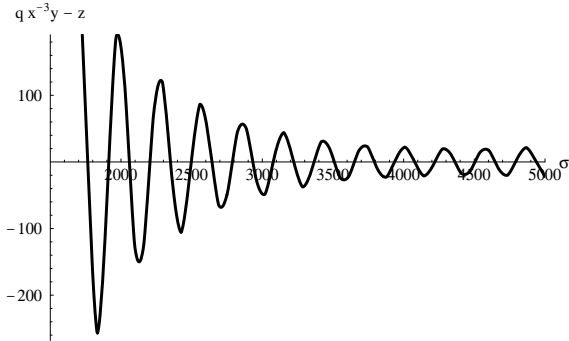


Fig. 5.— Behavior of the boundary condition at surface (equation (25)) for **TPM** model as a function of σ in μHz .

The equations (1) and (2) are very convenient for the analytical discussion, but for the numerical computations we use the more appropriate form:

$$\frac{dy}{dz} = \frac{l+1}{x} \left[-y + \frac{l}{\omega^2} z \right] + \frac{x}{\Gamma_1} \frac{GM_\odot \rho}{R_\odot P} \left(\frac{q}{x^3} y - z \right) \quad (17)$$

$$\frac{dz}{dx} = \frac{1}{x} [\omega^2 y - lz] + R_\odot A \left(\frac{q}{x^3} y - z \right) \quad (18)$$

where we have put:

$$\frac{r}{R_\odot} = x \quad (19)$$

$$\frac{m}{M_\odot} = q \quad (20)$$

$$\frac{\delta(r)}{R_\odot} = x^{l-1} y \quad (21)$$

$$\frac{R_\odot P'}{GM_\odot \rho} = x^l z \quad (22)$$

$$\frac{R_\odot^3 \sigma^2}{GM_\odot} = \omega^2 \quad (23)$$

The regularity condition at the centre, first requires that

$$\omega^2 y - lz = 0 \quad (24)$$

and second, the cancellation at the surface of the lagrangian perturbation of the pressure which can be written down as:

$$\frac{q}{x^3} y - z = 0 \quad (25)$$

In order to determine the solution uniquely, we impose the normalizing condition

$$y = 1 \quad (26)$$

at the centre. With a trial value for ω^2 we integrate equations (17) and (18), with initial conditions (24) and (26) using Runge-Kutta method, with a step size taken from a paper of Christensen-Dalsgaard, equation (A.55) [Christensen-Dalsgaard and Mullan,1994]. Usually this solution does not satisfy equation (25) and a new integration is performed with another value of ω^2 . This procedure is repeated until equation (25) is satisfied, using a Newton-Raphson method to improve the value of ω^2 .

3.1. Phase Diagram

The radial displacement $\delta(r)$ and the pressure perturbation P' are periodic space functions; the variables $v(r)$ and $w(r)$ vary strongly from the center to the surface, then it is impossible to plot them directly along the axes. However, the most appropriate functions:

$$\xi = \pm \log_{10} \left(1 + \left| \frac{\delta(r)}{R_\odot} \right| \right) \quad (27)$$

$$\zeta = \pm \log_{10} \left(1 + \left| \frac{R_\odot P'}{GM_\odot \rho} \right| \right) \quad (28)$$

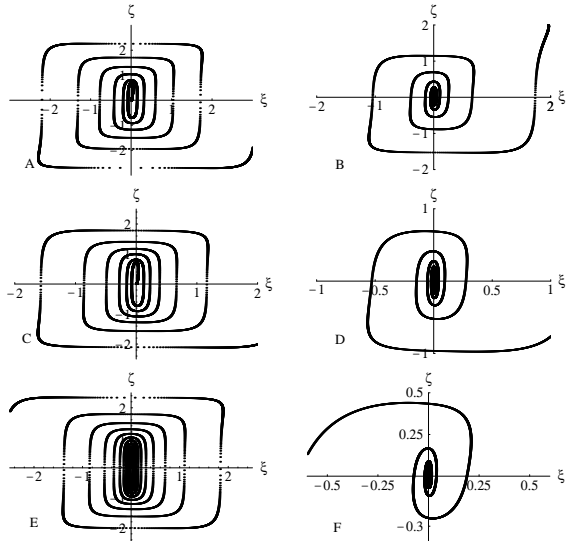


Fig. 6.— Some p -modes for polytropic models. Figures **A** and **B** corresponds to p_{12} modes with $\sigma_{n,l} = \sigma_{12,2} = 1796.89 \mu\text{Hz}$ and $\sigma_{12,4} = 1880.45 \mu\text{Hz}$ respectively for the $n = 3$ one polytrope model. **C** ($\sigma_{12,2} = 2059.86 \mu\text{Hz}$), and **D** ($\sigma_{12,4} = 2165.79 \mu\text{Hz}$), are the same modes but in **BPM**, while **E** ($\sigma_{21,2} = 3368.89 \mu\text{Hz}$) and **F** ($\sigma_{21,5} = 3531.43 \mu\text{Hz}$) represents the p_{21} mode for **TPM**.

have been plotted (27) and (28) in each axis of the *Fig.6*; their signs are chosen according to the signs of the variables $\delta(r)$ and P' . The number of intersections of each curve with the ordinate axis in *Fig.6* (the origin excluded) is equal to the order of the mode. The sense of rotation of this curves is a characteristic feature for the **p-modes** [Scuflaire,1974].

4. Conclusion

Although we do not use an atmosphere model and the input physics is described by a multipolytropic structure, the modes obtained from the **TPM** are close to the observacional data. We show in *Fig.7* a comparison with GOLF data⁵, showing an agreement within a few percent (roughly between 4.5% and 7%) up to a radial order of 30. However, we can see that the **TPM** model is more reliable than the **BPM** one for all radial orders considered ($n_r = 10$ to 30), being

⁵taken from www.medoc.ias.u-psud.fr/golf.html

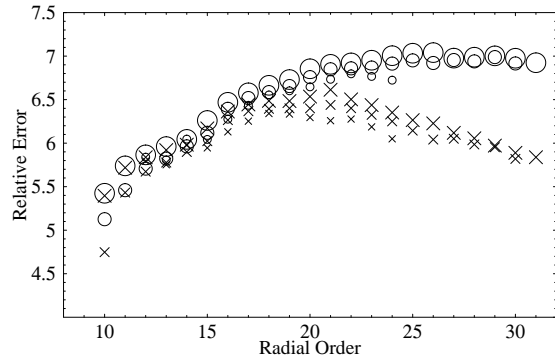


Fig. 7.— Comparison of **GOLF** data with those of the **TPM** (crosses) and the **BPM** (open circles) models for $l = 2, 3, 4$; sizes of circles and crosses are inversely proportional to l . The *Relative Error* value is given by $\frac{\sigma_{MODEL} - \sigma_{GOLF}}{\sigma_{GOLF}} \times 100\%$

noticeable at the higher ones.

REFERENCES

- Bahcall, M., Pinsonneault, M.:1995, *Rev.Mod.Phys*, **67**, 781 and astro-ph/0010346 (**SSM-BP2000**)
- Chandrasekhar, S.:1939, *An Introduction to the Study of Stellar Structure*, Dover Publications, Chicago
- Christensen-Dalsgaard J., Mullan, D.J.:1994, *M.N.R.A.S.*, **270**, 921
- Cowling, T.G.:1941, *M.N.R.A.S.*, **101**, 367
- Hendry, A.:1993, *Am.J.Phys*, **61**, 10
- Kopal, Z.:1949, *ApJ*, **109**,509
- Ledoux, P., Walraven, T.:1958, *Handbuch der Physik Vol LI*, Springer Verlag, Berlin
- Mullan, D., Ulrich, R.:1988, *ApJ*, **331**, 1013
- Pinzón, G., Calvo Mozo, B.:2001, astro-ph/0102429
- Scuflaire, R.:1974, *A&A*, **36**, 107
- Tassoul, M.:1980, *ApJss*, **43**, 469
- Unno, W., Osaki, Y., Ando, H., Saio, H., Shibahashi, H.:1989, *Nonradial Oscillations of Stars*, University of Tokio Press, Tokio

This 2-column preprint was prepared with the AAS L^AT_EX macros v5.0.